IP-BBSR-93-40
11-9-93
Fermilab Library
0 1160 0031850 5
IP-BBSR-93-40

ELECTRON-PHONON INTERACTION, PHONON RESPONSE AND RAMAN SCATTERING IN A CORRELATED SUPERCONDUCTOR[1]

SURJYO N. BEHERA[2] and PETER ENTEL

Theoretische Tieftemperaturphysik
Universität-GH-Duisburg, 47048 Duisburg, Germany

and

DEBANAND SA

Institute of Physics, Bhubaneswar-751 005, Orissa, India

ABSTRACT

A brief summary of some of the properties of the copper oxide superconductors is presented with emphaysis on the anomalous behaviour of the Raman scattering data. The temperature dependence of the Raman scattering cross section is calculated from first principles assuming that the normal state of these systems is a correlated metal and that superconductivity is described by the correlation bag model. It was demonstrated that the correlated metallic state exhibits the marginal Fermi liquid behaviour. A new mechanism of charge carrier-phonon interaction involving the decay of the phonon into a quasiparticle pair, due to the breaking of the local bonds in the normal state, is postulated and the phonon response of the system is calculated. The temperature dependence of the phonon frequencies and their widths arising due to their self energies are shown to be strongly influenced by this new mechanism of interaction. The calculated Raman spectrum reproduces the observed constant background intensity due to scattering by charge carriers. It also predicts the softening of the phonon frequencies and broadening of their peaks in the normal state, in qualitative agreement with the recent measurements.

1. Introduction

Since the discovery of high temperature superconductivity by Bednorz and Müller [1] in $La_{2-x}Ba_xCuO_4$ (the so called 214 system with a transition temperature (T_c) of $\sim$ 35 K), sveral other families of copper oxides and other systems have been discovered, and the transition temperature has been raised to a highest of 134 for the system $HgBa_2Ca_2Cu_3O_{8+x}$ (Hg-1223). To make a brief mention of these systems, among the copper oxides, there are the 123 system $YBa_2Cu_3O_{7-\delta}$ with a T_c of 90 K, the Bismuth 2212 and 2223 systems $Bi_2Sr_2CaCu_2O_8$, $Bi_2Sr_2Ca_2Cu_3O_{10}$ with T_c's of 80 and 110 K and finally the families of thallium 2223 i.e. $Tl_2Ca_2Ba_2\ Cu_3O_{10}$ with the T_c of 125 K which were discovered in quick succession. All the above mentioned cuprates are grouped as the hole-doped systems as the charge carriers in these are holes. The discovery of these cuprate supercondocturs broke the liquid nitrogen barrier, since they have T_c's above the liquid nitrogen temperature. This development was followed by the discovery of yet another system $(Nd_{1-x}Ce_x)_2CuO_4$ with a T_c of 30 K, which is an electron doped superconductor. For some time it was thought that the presence of copper in the system was a prerequisite for producing a high T_c superconductor, till superconductivity was found in the system $Ba_{1-x}K_xBiO_3$ with a T_c of $\sim$30 K. Obviously this is a non-copper system and its properties differ considerably from those of the cuprates. The latest addition to the list of high temperature superconductors are the so called bucky ball superconductors or the alkali doped fullerides with T_c's of 18 K for K_3C_{60}, 28 K for Rb_3C_{60} and 33 K for Cs_2RbC_{60}. Again these systems have very different properties than the cuprates. Here we shall be concerened only with the cuprates.

The basic properties of all the cuprates can be briefly summarized by going through their phase diagrams, which depict the different phases of the material as a function of the dopant concentration (or equivalently the oxygen content). Since all the cuprates have similar phase diagrams, we discuss only the one for the 214 system which is depicted in Fig. 1. In the figure the different transition temperatures are plotted as a function of the dopant concentration x. The pure material La_2CuO_4 ($x = 0$) undergoes a structural change from the tetragonal to the orthorhombic phase at a rather high temperature. On lowering the temperature it becomes an antiferromagnet below the Néel temperature (T_N) of 350 K; and it is an insulator. At the outset it is even difficult to understand why the pure material is an insulator. On matching the valence of the stoichiometric compound it is clear that copper exists in the Cu^{2+} state and has an atomic structure of $3d^9$. Since the d-shell can accomodate 10 electrons, there is a partialy filled d level in the system, and this will give rise to partially filled band when the solid is formed. Therefore, band theory predicts this system to be a metal. Even if we try to refine the picture by taking into account the crystal field splitting of the d level and so on, one still ends up with a half filled valence band, which should be a metal. The only way that the system could become an insulator is by invoking strong electron correlations which will produce antiferromagnetism (AF) in the system, and thereby split the half-filled band into two bands due to the doubling of the periodicity. This suggests that we have a strongly correlated system at hand, which was first recognized by Anderson [2]. On doping the system, the Néel temperature decreases very rapidly, and the long range AF order vanishes, when the dopant concentration is of the order of an atomic per cent. On further doping there results a disordered magnetic state, sometimes denoted the spin-glass state, and the system continues to be an insulator. Of course doping creates holes which are the charge carriers in the insulator, simply because the divalent alkaline earth metal atom (Ba or Sr) replaces the trivalent La atom. When the dopant concentration increases to about 5 at % the system undergoes a transition from the insulating to the metallic state

[1]Transcript of the talk presented by one of us (S.N.B.) at the *International Symposium on Local Order in Condensed Matter Physics* held at Jekyll Island, Georgia, U.S.A. during June 14-17, 1993.
[2]Permanent address: Institute of Physics, Bhubaneswar-751 005, Orissa, India

and on lowering the temperature superconductivity appears in the system. The insulator-metal transition is again believed to be a characteristic feature associated with strongly correlated charge carriers in the system. The SC transition temperature at first increases with x, reaches a saturation, then decreases, finally vanishing for $x \approx 0.3$ as can be seen from Fig. 1. Beyond this dopant concentration, the system is known to be a good Fermi liquid like metal. On the other hand the range of the dopant concentratin $0.05 \leq x \leq 0.3$, where SC has been observed, the normal state corresponds to a bad metal. To distinguish between the good and the bad metallic states, the behaviour of the resistance as a function of the temperature in the three different regions marked 1, 2, 3 in the phase diagram is shown schematically in the inset of fig. 1. In the good metallic region (3) the resistance shows the expected linear temperature dependence at high temperatures due to scattering by phonons, the temperature independent behaviour at low temperatures corresponding to the residual resistance and T^2 dependence in the intermediate region corresponding to the scattering by Coulomb interaction. In region (1) the temperature dependence of the resistance is typically that of a semiconductor. In contrast in the region of bad metal (2) the resistance shows a linear temperature dependence from high down to the lowest temperatures. This linear temperature dependence happens to be a chaacteristic feature of all the cuprate systems and is believed to be caused by a mechanism of scattering intrinsic to these systems. A proper understanding of this anomalous temperature dependence of the resistance in the metallic state is recognized to be the key feature to a proper understanding of the mechanism of superconductivity in these systems. This follows from a rather universal thumb rule that bad metals are good superconductors. In the conventional superconductors the resistance in the metallic state is caused by phonons and so also is the mechanism for superconductivity. So it is natural to believe that in the cuprates, whatever causes the resistance in the bad metallic state, should also be responsible for the mechanism of pairing of charge carriers and hence superconductivity. It is not only the resistance but there are many other properties which show anomalous behaviour in the bad metallic state. One such property is the Raman scattering cross section, a close examination of which reveals the nature of the bad metallic state.

In section 2 we discuss the interesting feature of the Raman data and point out the inferences that one can draw from it regarding the normal as well the superconducting state. An interpretation of the data requires the calculation of the Raman scattering cross section. This in turn necessitates a model for the normal as well as the superconducting states. Such a model has been developed in [3], following the evolution of the system with dopant concentration as given by the phase diagram. The essential features of the models for the normal and the superconducting states will be discussed in section 3. Since in these systems the Raman spectrum arises due to scattering by charge cariers as well as phonons: it will be important to know how the phonons couple to the charge carriers. It was shwon earlier [3] that there are two different ways in which the phonons interact with the charge carriers in the system. Again the basic mechanisms for the charge carrier-phonon interactions and the nature of the phonons in these systems will be presented in section 4, along with the calculation of the phonon response and their spectral density functions, the later being the quantities measured in a Raman experiment. Finally section 5 is devoted to a discussion of the results.

2. The Raman Data

Raman scattering [4] from the copper oxide superconductors has shown several unusual features which provided much usful information about the normal as well as the superconducting states. A summary of the essential features is given below:

(i) In the the normal state, a rather large but constant background intensity has been observed at all frequencies up to the highest measured frequency as can be seen from Fig. 2, which depicts the spectrum for the Bismuth (2212) [5] system. This is a general feature of all the copper oxide superconductors. This background intensity has been attributed to the scattering by the charge carriers in the system and it dictates a particular form for the frequency and temperature dependence of the polarizability of the medium as can be seen from the arguments given below: The Raman intensity is proportional to a thermal factor times the imaginary part of the polarizability at zero wave vector $\Pi(\mathbf{q} = 0, \omega)$ and is given by

$$I \approx \left(1 - e^{-\beta\omega}\right)^{-1} \operatorname{Im}\Pi(\mathbf{q} = 0, \omega). \tag{1}$$

The high and low temperature behaviour of the thermal factor is

$$\left(1 - e^{-\beta\omega}\right)^{-1} \approx \begin{cases} 1 & \text{for} \quad \omega \gg T \\ T/\omega & \text{for} \quad \omega \ll T \end{cases} \tag{2}$$

Since the intensity is a constant independent of frequency and temperature it follows from eqns. (1) and (2) that the imaginary part of the polarizability must have the following form

$$\operatorname{Im}\Pi(\mathbf{q} = 0, \omega) = \begin{cases} S_0 & \text{for} \quad \omega \gg T \\ S_0(\omega/T) & \text{for} \quad \omega \ll T \end{cases} \tag{3}$$

This particular frequency and temperature dependence of the polarizability is the basis of the phenomenological marginal Fermi liquid theory for the cuprates proposed by Varma et al. [6]. Recently more careful analysis of the scattering intensity by charge carriers in the case of the (214) [7] and the (123) [8] systems has revealed that the intensity background persists even in the insulating as well as the highly doped good metallic states.

(ii) Usually at low frequencies the phonon peaks ride over the constant intensity background of the Raman spectrum. The number of phonon peaks seen may differ form one Cuprate to the other. In the (123) system [4] three prominent phonons having frequencies of 116, 340 and 504 cm^{-1} have been observed (see Fig. 3) and identified to be associated with the out of phase vibrations of the Ba, in plane Oxygen and the apex Oxygen atoms, respectively. Some of these show the Fano line shape indicating a strong coupling to the charge carriers in the system.

(iii) On lowering the temperature below the superconducting transition temperature the 116 cm^{-1} phonon sharpens while the 340 cm^{-1} phonon shows anomalous softening while its width increases. All these features again indicate a strong coupling to the charge carriers in the superconducting state [9].

(iv) In the superconducting state the constant background intensity is suppressed at low frequencies while it develops a broad peak with its maximum around 490 cm^{-1}. The suppression of the intensity in the low frequency region is interpreted as being due to the appearance of the superconducting gap. However, the slow linear rise of the intensity in this region also indicates the presence of a finite density of states inside the superconducting gap.

(v) The broad peaking of the background intensity in the SC state is a puzzling feature. While some peaking is expected from the redistribution of the density of states in the vicinity of the SC gap, the occurrence of the peak maximum at a rather high frequency and its invariance with samples of varying T_c point to the fact that it may be a normal state feature.

(vi) Recently the shift in the phonon frequency and change in their width has been studied more carefully as a function of the oxygen content of the sample [10]; which shows the softening of the high frequency mode at a temperature much higher than T_c in a low T_c sample with low oxygen content. This is indicative of the presence of a gap even in the normal state of the system. A theoretical analysis [11] of all these puzzling features will throw light on the nature of the normal as well as the SC states of the cuprates.

In a metal normally Raman scattering proceeds as follows: The incident photon excites an electron-hole pair, which finally recombines to emit the scattered photon. Simultaneously, the electron or hole can emit or absorb a phonon because of the electron-phonon interaction as depicted in Fig. 4a [12]. However, only the zero momentum ($\mathbf{q} = 0$) phonons will take part in the process because of the conservation of momentum. The $\mathbf{q} = 0$ phonon can further acquire a self energy due to its coupling to the quasiparticles of the ground state of the system as shown in Fig. 4b. Thus the phonon response of the system is capable of providing informaton about the ground state, because of which Raman scattering can be successfully used to probe both the normal as well as the SC states as demonstrated in 1980 [13] for the first time. The Raman intensity is proportional to the sum the imaginary parts of the polarizabilities and the phonon spectral density functions, and is given by

$$I \approx \left(1 - e^{-\beta\omega}\right)^{-1} \left[\sum_i \mathrm{Im}\,\chi^i(\omega) + \sum_i \mathrm{Im}D^i(0,\omega)\right] . \tag{4}$$

where $\chi^i(\omega)$'s are the different response functions of the system and the phonon spectral density functions are the imaginary parts of the phonon Green's functions $D^i(0,\omega)$. Obviously the evaluation of the response functions $\chi^i(\omega)$ as well as the phonon self energy in the normal and the SC state requires proper models for these states.

3. The Correlated Metallic State and Superconductivity

The metallic state in the cuprates evolves from that of the AF-insulator on increasing the dopant concentration. It was pointed out in the introduction that the properties of the pure system can be understood only when the strong electron correlations are taken into account. Since these are highly anisotropic systems with the action taking place in the CuO_2 planes a realistic model for the cuprates should involve the orbitals of one Cu and two O-atoms which constitute the unit cell in this plane. The Cu d-orbitals are expected to exhibit strong correlations. If one takes only those orbitals which lie in the CuO_2 plane it will lead to a three or a five band model [14]. However, for simplcity we consider only the one band Hubbard model, as the one appropriate to take care of strong correlations in the cuprates. The Hamiltonian for the Hubbard model is [15]

$$\mathcal{H} = \sum_{ij,\sigma} t_{ij} c^\dagger_{i\sigma} c_{j\sigma} + U \sum_i n_{i\uparrow} n_{i\downarrow} , \tag{5}$$

where the symbols have their usual meaning. In the limit of the intraatomic Coulomb repulsion $U \to \infty$, the Hubbard Hamiltonian transforms into the Heisenberg antiferromagnetic exchange interaction [16], given by

$$\mathcal{H} = J \sum_{\langle ij \rangle} \left(\mathbf{S}_i \mathbf{S}_j - \frac{1}{4} n_i n_j \right) , \tag{6}$$

where the kinetic exchange integral $J = 2t^2/U$. This Hamiltonian describes the AF-insulating ground state of the pure system. On doping, the long range AF order disappears, giving way to a disordered magnetic state, which could be the insulating resonating valence bond (RVB) state described by the Hamiltonian [17]

$$\mathcal{H} = -J \sum_{\langle ij \rangle} b^\dagger_{ij} b_{ij} , \tag{7}$$

where

$$b^\dagger_{ij} = \frac{1}{\sqrt{2}} \left(c^\dagger_{i\uparrow} c^\dagger_{j\downarrow} - c^\dagger_{i\downarrow} c^\dagger_{j\uparrow} \right) \tag{8}$$

is the valence bond operator. This is a spin liquid like state consisting of nearest neighbour spin pairs. In the mean field approximation the Hamiltonian of eqn. (7) can be diagonalized and be described by a non-vanishing value of the valence bond order parameter $\Delta = \langle b^\dagger_{ij} \rangle$. At this stage because of the presence of a small number of holes in the system there can be charge and spin seperation and the elementary excitations will be the holons and the spinons [18]. However, because of the disorder the states are localized and there is no possibility for the charge transport in the system. On further increasing the dopant concentration the RVB metallic state results, which is described by the mean field Hamiltonian

$$\mathcal{H}_0 = -t' \sum_{ij,\sigma} c^\dagger_{i\sigma} c_{j\sigma} - J\Delta \sum_{\langle ij \rangle} (b_{ij} + b^\dagger_{ij}) . \tag{9}$$

t' being a modified hopping integral proportional to the dopant concentration. The presence of mobile holes in this state will self consistently generate strong fluctuations of the valence bond because of the possibility of virtually breaking and making the bonds as the holes move. Therefore, the holes are expected to couple strongly with the fluctuations over the mean field. The fluctuations in the valence bond operators can be written as

$$b^\dagger_{ij} = \Delta - \delta^\dagger_{ij} . \tag{10}$$

where $\tilde{b}^{\dagger}_{ij}$ is the fluctuating part of the operator. The interaction Hamiltonian is obtained by substituting eqn. (10) into eqn. (7) and is given by

$$\mathcal{H}_I = -J \sum_{(ij)} \left(b^{\dagger}_{ij} \tilde{b}_{ij} + \tilde{b}^{\dagger}_{ij} b_{ij} \right) . \tag{11}$$

The quanta of the fluctuations over the mean field are just the collective modes of the system describing the oscillations of the amplitude and the phase of the order parameter. Hence the operators corresponding to the fluctuations can be decomposed into bosonic anihilation and creation operators while the original valence bond operators are expressed in terms of the hole anihilation and creation opeators using eqn. (8). Then the interaction Hamiltonian of eqn. (11) describes the interaction of quasiparticle pairs with the bosonic degrees of freedom. This interaction given by eqn. (11) together with the mean field Hamiltonian of eqn. (9) will describe the *correlated metallic* state as was first pointed out in [3]. The other characteristics of the correlated metal are the following: (i) The presence of valence bonds in the metallic state opens up a gap over regions of the Fermi surface. With increasing dopant concentration the gap region of the Fermi surface decreases. (ii) The elementary excitations of the system are regular Fermions carrying both spin and charge. (iii) The interaction of eqn. (11) will renormalize the quasiparticles of the system, which will acquire self energy due to the fluctuations. The propagator for the quanta of the fluctuations is the pair susceptibility function. This latter quantity when calculated using the mean field Hamiltonian (9) is given by [11]

$$\chi^{p-p}(0,\omega) = \sum_{\mathbf{k}} \frac{4(\varepsilon_{\mathbf{k}} - \mu)^2}{E_{\mathbf{k}}} \frac{\tanh(\beta E_{\mathbf{k}}/2)}{(\omega^2 - 4E_{\mathbf{k}}^2)} , \tag{12}$$

where

$$E_{\mathbf{k}} = \left[(\varepsilon_{\mathbf{k}} - \mu)^2 + \Delta_R^2 \right]^{1/2} . \tag{13}$$

$\Delta_R = -J\Delta$ being the gap parameter of the metallic state. In the region of $(\omega/2\Delta_R)^2 > 1$, the frequency and temperature dependence of the imaginary part of $\chi^{p-p}(0,\omega)$ is given by

$$\mathrm{Im}\,\chi^{p-p}(0,\omega) = -\frac{\pi N(0)}{4} \frac{[(\omega/2\Delta_R)^2 - 1]^{1/2}}{(\omega/2\Delta_R)} \begin{cases} (\omega/4T) & \text{for} \quad \omega < 4T \\ 1 & \text{for} \quad \omega > 4T \end{cases} \tag{14}$$

where $N(0)$ is the density of states at the Fermi energy. In the limit of vanishing normal state gap ($\Delta_R \to 0$) eqn. (14) reduces to

$$\mathrm{Im}\,\chi^{p-p}(0,\omega) = -\frac{\pi N(0)}{4} \begin{cases} (\omega/4T) & \text{for} \quad \omega < 4T \\ 1 & \text{for} \quad \omega > 4T \end{cases} \tag{15}$$

which is identical in form to eqn.(3) and is the Varma-polarizability. Therefore, the fluctuations over the mean field renormalize the quasiparticles so that the marginal Fermi liquid behaviour is generated. Because of this the theory of the correlated metallic state is capable of explaining many of the anomalous properties of the normal state of the cuprates. However, it should be pointed out that the marginal Fermi liquid like behaviour is also generated in the nested Fermi liquid theory [19] as well as in theories with strong electron-phonon coupling [20] and those with Fermi liquids involving two-dimensional plasmon exchange [21].

The density response function (particle-hole polarizability) for the correlated metallic state can also be calculated [3,11]. This will contribute to the phonon response as well as to the scattering by the charge carriers. In the case of a normal Fermi liquid like metal, the density response function is given by the Lindhard function. For the calculation of the Raman intensity we have to evaluate the imaginary part of the Lindhard function at $\mathbf{q} = 0$; and this quantity simply goes to zero. Therefore, there is no scattering by charge carriers in normal metals. However, in the model of the correlated metallic state, there will be a finite contribution to the density response function at $\mathbf{q} = 0$. because of the presence of local pairs in the system. This contribution will be proprtional to the gap (Δ_R) in the normal state and is given by [3,11]

$$\chi^{p-h}(0,\omega) = \Delta_R^2 \sum_{\mathbf{k}} \frac{\tanh(\beta E_{\mathbf{k}}/2)}{E_{\mathbf{k}}(\omega^2 - 4E_{\mathbf{k}}^2)} . \tag{16}$$

The imaginary part of $\chi^{p-h}(0,\omega)$ will contribute to the light scattering by charge carriers. The temperature dependence of this quantity for different ranges of frequency are given below. For $(\omega/2\Delta_R)^2 > 1$

$$\mathrm{Im}\,\chi^{p-h}(0,\omega) = -\frac{\pi N(0)}{4} \frac{1}{(\omega/2\Delta_R)} \frac{1}{[(\omega/2\Delta_R)^2 - 1]^{1/2}} \begin{cases} (\omega/4T) & \text{for} \quad \omega < 4T \\ 1 & \text{for} \quad \omega > 4T \end{cases} \tag{17}$$

and for $(\omega/2\Delta_R)^2 < 1$

$$\mathrm{Im}\,\chi^{p-h}(0,\omega) = \frac{N(0)}{4} \frac{1}{[1 - (\omega/2\Delta_R)^2]^{1/2}} \cdot \ln \left| \frac{[1 - (\omega/2\Delta_R)^2]^{1/2} - 1}{[1 - (\omega/2\Delta_R)^2]^{1/2} + 1} \right| \begin{cases} (2\Delta_R/4T) & \text{for} \quad \omega < 4T \\ 1 & \text{for} \quad \omega > 4T \end{cases} \tag{18}$$

Unlike the pair polarizability (eqn. (14)), the imaginary part of the density response function vanishes in the limit of $\Delta_R \to 0$ as can be seen from eqn. (17). However, for finite Δ_R, there will be a contribution to the Raman intensity due to charge carrier scattering coming from the density response function. Besides eqn. (16) will also contribute to the phonon response.

Within this model of the correlated metallic state superconducting pairing of the quasiparticles is generated by an effective interaction mediated by the exchange of the collective modes of the system: as has been shown in detail in [3]. Such a model for superconductivity is called the correlation bag model which is essentially dictated by the thumb rule mentioned in the introduction. The particle-hole and the particle-particle (or pair) polarizabilities in the superconducting state can also be calculated [3,11] to

compute the Raman intensities.

4. The Charge Carrier-Phonon Interaction and the Phonon Response

It was mentioned in the introduction that the Raman intensities are determined by scattering due to charge carriers as well as the phonons. The phonon contribution is proportional to its spectral density function as given by eqn. (4), and its evaluation requires the calculation of the phonon self energy. The phonon response of the system will therefore depend on the nature of the charge carrier-phonon interaction as well as the ground state of the charge cariers in the system. Usually the displacements of the ions ($\mathbf{u}_i$) from the equilibrium position modulates the hopping integral t_{ij} in eqn. (5) which gives rise to the normal electron-phonon interaction

$$\mathcal{H}^{(1)}_{c-p} = g \sum_{(i,j)} c^{\dagger}_{i\sigma} c_{j\sigma} (\mathbf{u}_i - \mathbf{u}_j) , \tag{19}$$

where a phonon decays by creating an electron-hole pair as shown in Fig. 5a. The phonon self energy due to this process comes from the density response function given by eqn. (16). On the other hand it was argued in [3] that the displacement of ions can modulate the kinetic exchange integral J_{ij} as well, which will give rise to the AF magnon-phonon interaction in the undoped insulating system. However, on doping the system, this interaction evolves with the increase in the dopant concentration as the ground state of the system changes. In the disordered magnetic state, since the ground state is an RVB insulator, this interaction will correspond spinon-phonon interaction. On further increasing the dopant concentration one ends up in the correlated metallic state, where the charge carrier-phonon interaction due to the modulation of J will essentially amount to the phonon creating or anihilating a pair as shown in Fig. 5b, and is given by

$$\mathcal{H}^{(2)}_{c-p} = g' \Delta \sum_{(i,j)} \left[b^{\dagger}_{ij} (\mathbf{u}_i - \mathbf{u}_j) + \text{h.c.} \right] . \tag{20}$$

The contribution of $\mathcal{H}^{(2)}_{c-p}$ to the phonon self energy, involves the pair correlation function as given by eqn. (12). In the correlated metallic state, both the mechanisms of interactions of eqns. (19) and (20) will be in operation, since the system is described by the Hamiltonian of eqn. (9). Furthermore, it is worth pointing out that the interaction of eqn. (20) vanishes if $\Delta = 0$, i.e. if there are no local pairs present in the ground state: therefore, this interaction is characteristic of the correlated metallic state alone.

It was pointed out in [3] that there are propagating as well as localized phonons present in the system. The localized phonons again owe its origin to the evolution of the correlated metallic state from the Néel ordered state. The presence of Néel ordereing will double the periodicity of the system which will thereby produce new phonon bracnches due to the halving of the Brillouin zone. On doping the system, the long range order vanishes and a disordered magnetic state results, which in turn is expected to localize those phonon branches which originated due to the Néel order. This is schematically depicted in Fig. 6. It is therefore expected that the localized phonons will interact with the charge carriers through the mechanism of eqn. (20) while the propagating phonon-charge carrier interaction is dominated by eqn. (19).

The Raman spectrum of the system will be dominated both by the propagating and the localized phonons and requires the calculation of their propagators which are given by

$$\mathcal{D}^{(i)}_{\mathbf{q}}(\omega) = \left(\omega^{(i)}_{\mathbf{q}}/\pi\right) \left[\omega^2 - \omega^{(i)2}_{\mathbf{q}} - \Pi^{(i)}(\mathbf{q},\omega)\right]^{-1} , \tag{21}$$

where $i = l, p$ denote the localized and the propagating modes, $\Pi^{(i)}(\mathbf{q},\omega)$ being their self energies arising out of the interactions $\mathcal{H}^{(i)}_{c-p}$ with $i = 2$ and 1, respectively. From the knowledge of the polarizabilities the spectral density functions for the different phonons can be calculated, which are given by

$$\begin{aligned} \mathcal{S}^{(i)}(0,\omega) &= -2\text{Im}\mathcal{D}^{(i)}_{\mathbf{q}=0}(\omega + i\eta^i) \\ &= \frac{-2\omega^i(2\omega\eta^i + \text{Im}\Pi^{(i)}(0,\omega)}{\pi\left([\omega^2 - \omega^{i2} - \text{Re}\Pi^{(i)}(0,\omega)]^2 + [2\omega\eta^i + \text{Im}\Pi^{(i)}(0,\omega)]^2\right)} \end{aligned} \tag{22}$$

where η^i are the intrinsic widths of the phonons with frequency ω^i and a temperature dependent shift of the phonon frequency and a change in width arises from the real and imaginary parts of the phonon self energies which are given by

$$\Pi^{(i)}(0,\omega) = \begin{cases} 2\pi\tilde{g}_l\Omega_0^2\,\tilde{\chi}^{p-p}(0,\omega) & \text{for} \quad i = l \\ 2\pi\tilde{g}_p\omega_0^2\,\tilde{\chi}^{p-h}(0,\omega) & \text{for} \quad i = p \end{cases} \tag{23}$$

where the dimensionless coupling constants are $\tilde{g}_l = (g'\Delta)^2 N(0)/\Omega_0$, $\tilde{g}_p = g^2 N(0)/\omega_0$; Ω_0 and ω_0 being the frequencies of the localized and propagating phonons and $\tilde{\chi}(0,\omega) = \chi(0,\omega)/(\pi N(0)/4)$. The pair and partile-hole polarizabilities are as given by eqns. (12) and (16). The real part of these functions are obtained from a Kramers-Kronig analysis of the imaginary parts [11].

5. Results and Discussion

The Raman intensity and its temperature dependence in the correlated metallic state can be calculated now using eqns. (4), (22), (14) and (17) in the range of frequencies $(\omega/2\Delta_R)^2 > 1$. Since the ground state of the system is not the usual Fermi liquid but a correlated state there will be contributions to the scattering by charge carriers coming from both the particle-hole and the pair polarizabilities. This is possible simply because an incident photon besides exciting an electron-hole pair can also break up a local pair and the scattered photon comes from the recombination of the electron and hole or the making of the local pair. In calculating the intensity from eqn. (4) it is further assumed that in the system under consideration there are only two phonons, one of the propagating and the other of localized nature. So the total intensity arises from the sum of the imaginary part of the two polarizabilities and the spectral density functions of the two phonons. Ther are several parameters which enter the calculation, e.g., the two dimensionless coupling constants for the phonons, $\tilde{g}_l$ and $\tilde{g}_p$, their intrinsic widths η^l, Ω_0 and η^p, ω_0, the ratio of the phonon frequency to the normal state gap $\omega_0/2\Delta_R$, the ratio of the two phonon frequencies ω_0/Ω_0 and of course the temperature $\omega/4T$. Figure 7 shows the variation of the Raman intensity with temperature for high

temperatures $\omega < 4T$ in the normal state, plotted as a function of the reduced frequency ω/ω_0 for a given set of parameters. The characteristic features of this plot are: (i) there is a temperature independent constant background intensity extending up to high frequencies and, (ii) the softening and broadening of both the propagating and localized phonon peaks with decreasing temperature, in the normal state. In fact, as pointed out in the introduction, recent Raman measurements [10] does show the softening and broadening of some phonons in the normal state. Figure 8 shows the same spectrum at low temperatures $\omega > 4T$, for the case of varying normal state gaps. Of course in the low temperature phase the spectrum is independent of temperature, and one can notice the constant intensity background extending up to a much higher frequency. In addition one can see a sharp jump in the spectrum corresponding to the value of the normal state gap. There is a qualitative resemblence of the calculated spectrum with the measured Raman spectrum for some cuprate superconductors. The spectrum in the superconducting state can also be calculated. The details of this calculations are presented in [11].

Acknowledgement

One of us (S.N.B.) would like to thank Prof. P. Entel for hospitality during his stay at the University of Duisburg and would like acknowledge the grant from SFB 166 for the financial support.

References

1. J.G. Bednorz and K.A. Müller, Z. Phys. B 64 (1986) 189.
2. P.W. Anderson, Science 235 (1987) 1196 and article in *Frontiers and Boarderlines in Many Particle Physics*. Varenna Lectures. Enrico Fermi School, edited by R. Broglia (North Holland, Amsterdam, 1987).
3. Debanand Sa and S.N. Behera, Physica C 203 (1992) 347.
4. S.L. Cooper and M.V. Klein, Comments in Cond. Mat. Phys. 15 (1990) 99; C. Thomsen and M. Cardona, in *The Physical Properties of High Temperature Superconductors*, Vol. I, edited by D.M. Ginsberg (World Scientific, Singapore, 1989).
5. T. Stauffer, R. Hackl and Müller, Solid State Commun. 75 (1990) 975.
6. C.M. Varma, P.B. Littlewood, S. Schmitt-Rink, E. Abrahams and A.E. Ruckenstein. Phys. Rev. Lett. 63, (1989) 1996; C.M. Varma, Int. J. Mod. Phys. B 3 (1989) 2083.
7. S. Sugai, Solid State Commun. 76 (1990) 365.
8. A.A. Maxsimov, A.V. Puchkov, I.I. Tartakovskii, D. Reznik, M.V. Klein, W.C. Lee and D.M. Ginsberg, JETP Lett. 56 (1992) 570.
9. R. Zehyer and G. Zwicknagl, Z. Phys. B 78 (1990) 175.
10. E. Attendorf, J.C. Irwin, R. Liang and W.N. Hardy, Solid State Commun. 80 (1991) 627 and E. Attendorf, X.K. Chen, J.C. Irwin, R. Liang and W.N. Hardy (1992), Simon Fraser Univsity Preprint.
11. Debanand Sa and S.N. Behera (1993), to be published.
12. M.V. Klein, in *Light Scattering in Solids*, Vol. 3, edited by M. Cardona and G. Guntherdort (Springer, Berlin, 1982).
13. R. Sooryakumar and M.V. Klein, Phys. Rev. Lett. 45 (1980) 660.
14. P. Entel, J. Zielinski, M. Matschke and S.G. Mishra, in *Electronic Correlation and Disorder Effects in Metals*, edited by S.N. Behera (World Scientific, Singapore, 1991); P. Entel and J. Zielinski, Phys. Rev. B 42 (1990) 307.
15. J. Hubbard, Proc. Roy. Soc. London A 276 (1963) 238.
16. K.A. Chao, J. Spalek and A.M. Oles, J. Phys. C 10 (1977) L271.
17. E. Baskaran, Z. Zou and P.W. Anderson, Solid State Commun. 63 (1987) 973.
18. S. Kivelson, D. Rokhasar and J. Sethna, Phys. Rev. B 35 (1987) 8865.
19. A. Virosztek and J. Ruvalds, Phys. Rev. B 42 (1990) 4064.
20. P. Entel (1993), talk presented in the present conference.
21. S. Bose (1993), talk presented in the present conference.

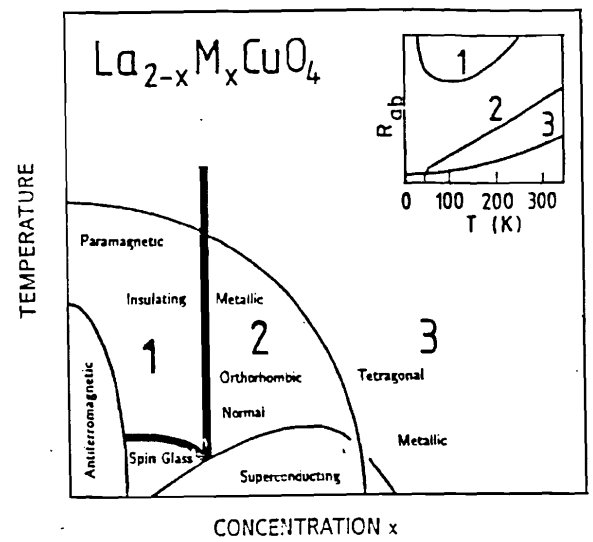

Figure 1: The schematic phase diagram for the $La_{2-x}Sr_xCuO_4$ system. The transition temperatures are plotted as function of the dopant concentration (x). The inset shows the temperature dependence of the resistance in the three regions marked 1, 2 and 3. For a discussion see the text.

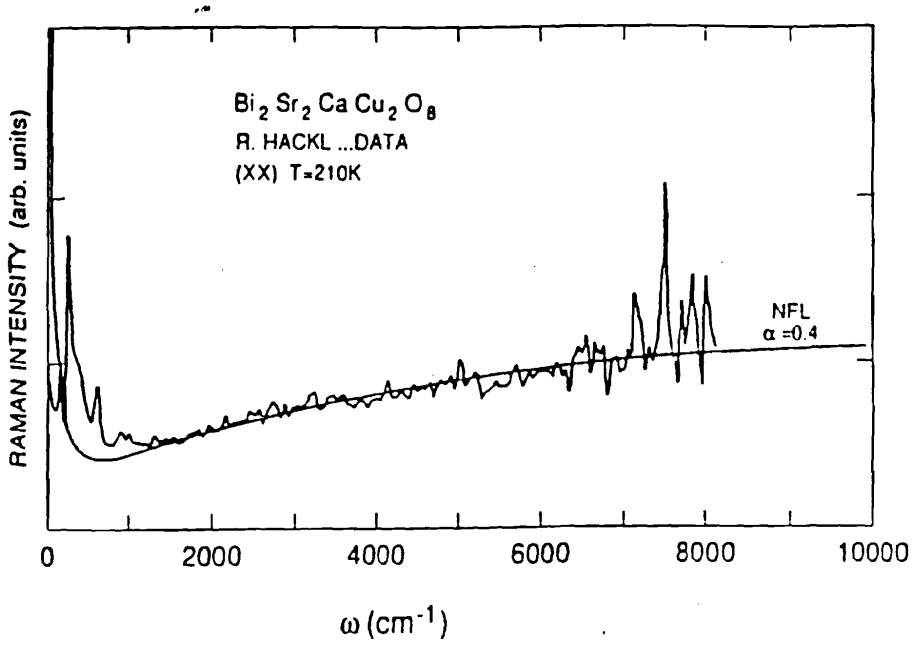

Figure 2: Raman spectrum for $Bi_2Sr_2CaCu_2O_8$ at 210 K, taken from Ref. [5].

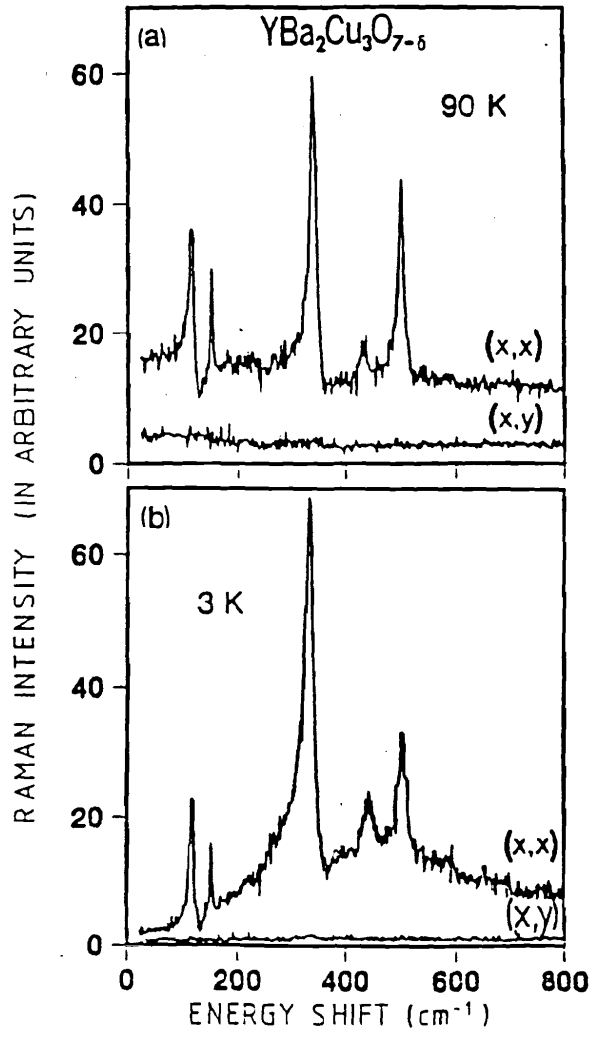

Figure 3: Raman spectrum of $YBa_2Cu_3O_{7-\delta}$ (a) at 90 K and (b) at 3 K from Ref. [4].

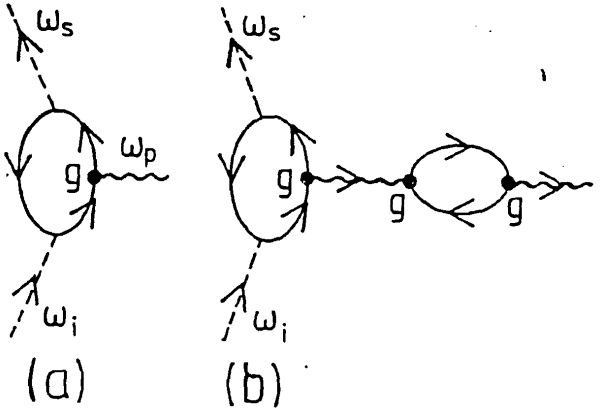

Figure 4: The process by which Raman scattering proceeds in a metal: (a) one phonon process, (b) probing the ground state through the phonon self energy.

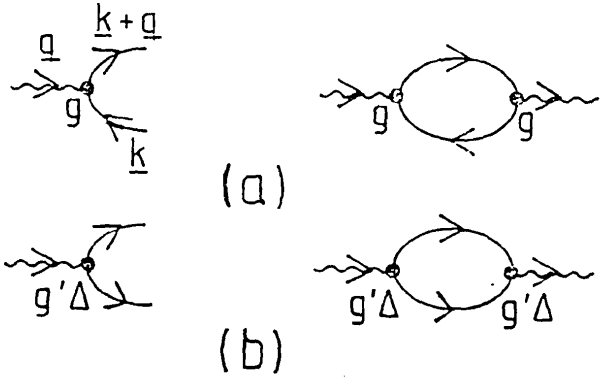

Figure 5: Process contributing to the charge carrier-phonon interaction: (a) the normal electron-phonon interaction and its contribution to phonon self energy in the lowest order, (b) the phonon interaction involving a local pair and its contribution to phonon self energy.

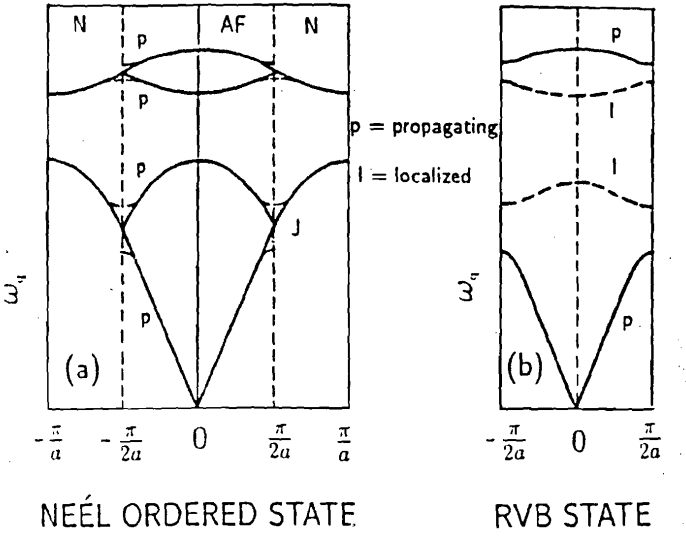

Figure 6: (a) The one-dimensional representatin of the phonon spectrum in the undoped Néel ordered state showing the appearence of new phonon branches due to the doubling of the periodicity, (b) in the doped system showing the localization of these phonon branches which appeared due to magnetic order. The localization is brought about by the disordered magnetic state.

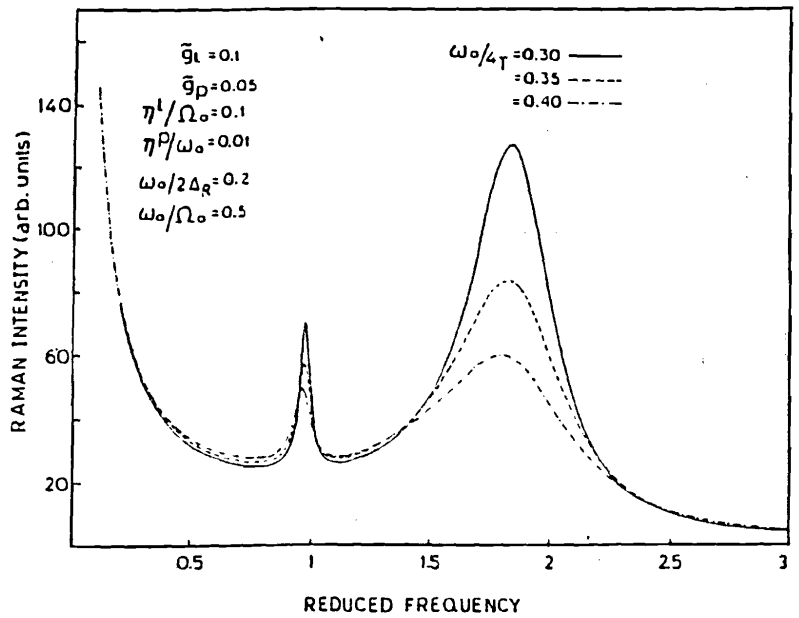

Figure 7: Raman intensity as a function of the reduced frequency (ω/ω_0) plotted for different values of the parameter ($\omega_0/4T$) in the high temperature region $\omega > 4T$. The values of the other parameters entering the calculation are $\tilde{g}^l = 0.1$, $\eta^l/\Omega_0 = 0.1$, $\tilde{g}^p = 0.05$, $\eta^p/\omega_0 = 0.01$, $\omega_0/2\Delta_R = 0.2$ and $\omega_0/\Omega_0 = 0.5$.

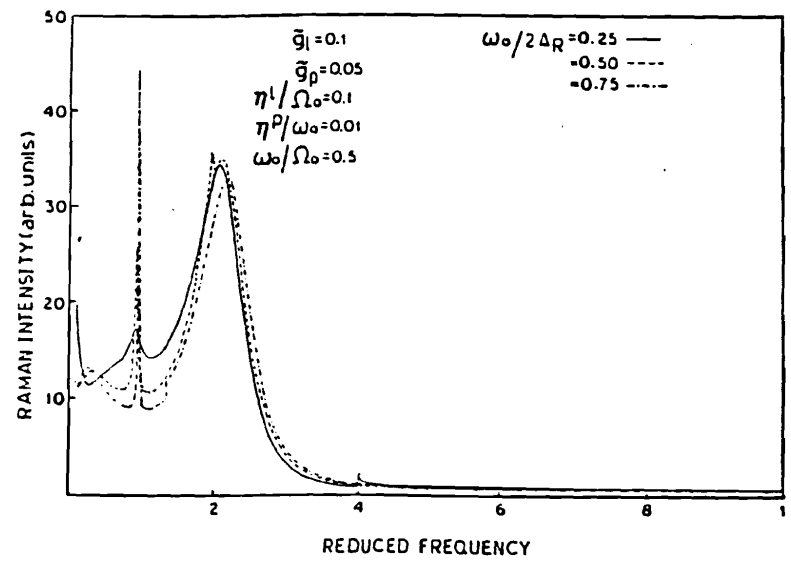

Figure 8: Raman intensity as function of reduced frequency plotted in the low temperature region $\omega > 4T$ for different values $\omega_0/2\Delta_R$. All the other parameters are the same as in Fig. 7.